

GA-A22449

FAST WAVE HEATING AND CURRENT DRIVE IN DIII-D DISCHARGES WITH NEGATIVE CENTRAL SHEAR

by

**R. PRATER, M.E. AUSTIN, F.W. BAITY, S.C. CHIU, R.W. CALLIS,
W.P. CARY, J.S. deGRASSIE, R.L. FREEMAN, C.B. FOREST,
S.W. FERGUSON, H. IKEZI, E.F. JAEGER, E. JOFFRIN, J.H. LEE,
Y.R. LIN-LIU, T.C. LUCE, M. MURAKAMI, C.C. PETTY, R.I. PINSKER,
D.A. PHELPS, M. PORKOLAB, D.W. SWAIN, and The DIII-D TEAM**

SEPTEMBER 1996

FAST WAVE HEATING AND CURRENT DRIVE IN DIII-D DISCHARGES WITH NEGATIVE CENTRAL SHEAR

by

R. PRATER, M.E. AUSTIN,* F.W. BAITY,† S.C. CHIU, R.W. CALLIS,
W.P. CARY, J.S. deGRASSIE, R.L. FREEMAN, C.B. FOREST,
S.W. FERGUSON,‡ H. IKEZI, E.F. JAEGER,† E. JOFFRIN,△ J.H. LEE,◇
Y.R. LIN-LIU, T.C. LUCE, M. MURAKAMI,† C.C. PETTY, R.I. PINSKER,
D.A. PHELPS, M. PORKOLAB,¶ D.W. SWAIN,† and The DIII-D TEAM

This is a preprint of a paper to be presented at the Sixteenth IAEA International Conference on Plasma Physics and Controlled Nuclear Research, October 7-11, 1996, Montreal, Canada, and to be published in *The Proceedings*.

*University of Maryland, College Park, Maryland.

†Oak Ridge National Laboratory, Oak Ridge, Tennessee.

‡Lawrence Livermore National Laboratory, Livermore, California.

△Association EURATOM-CEA, Cadarache, France.

◇University of California, Los Angeles, California.

¶Massachusetts Institute of Technology, Cambridge, Massachusetts.

Work supported by
the U.S. Department of Energy under Contract Nos.
DE-AC03-89ER51114, DE-AC05-96OR22464, W-7405-ENG-48,
and Grant Nos. NDE-FG05-86ER5 and DE-FG03-89ER53266

GA PROJECT 3466
SEPTEMBER 1996

F1-CN-64/E-1

**FAST WAVE HEATING AND CURRENT DRIVE IN DIII-D
IN DISCHARGES WITH NEGATIVE CENTRAL SHEAR**

ABSTRACT

The noninductive current driven by fast Alfvén waves (FWCD) has been applied to discharges in DIII-D with negative central shear. Driven currents as high as 275 kA have been achieved with up to 3 MW of fast wave power with the efficiency and profile as predicted by theory-based modeling. When counter-current FWCD was applied to discharges with negative central shear, the negative shear was strengthened and prolonged, showing that FWCD can help to control the current profile in advanced tokamak discharges. Under some conditions in negative central shear, the plasma spontaneously makes a transition into a regime of improved performance, with a reduction in both the ion and the electron heat diffusivities. Up to 3 MW of fast wave power has been successfully coupled into H-mode discharges with large edge localized modes through use of an innovative decoupler/hybrid power splitter combination.

1. INTRODUCTION

Discharges with weak or negative central magnetic shear (NCS) in DIII-D are characterized by access to improved performance: normalized beta has reached 4.0 while the confinement remains very high, $H \approx 4.5$, with high power neutral heating above a threshold value [1]. These current profiles with negative shear have been generated using heating by neutral beams during the current ramp phase of the discharge in order to raise the conductivity of the plasma [2,3]. Current profiles generated in this way decay into normal (positive) shear discharges on a resistive time scale; to sustain the high performance phase, it is necessary to maintain negative shear by noninductive current drive in combination with bootstrap current. The present work describes the application of fast wave current drive (FWCD) for this purpose.

Discharges with NCS with an L-mode edge are well suited for FWCD experiments. Mild neutral beam heating of 3 to 5 MW during the current ramp keeps the electron temperature high enough, typically above 2.5 keV, that the fast waves are effectively damped by the thermal electrons. At the same time, the density is low enough, typically below $3 \times 10^{19} \text{ m}^{-3}$, that the noninductively driven currents can be moderately high. Equally important, sawteeth are absent since the safety factor q is everywhere greater than unity; this allows application of the technique developed by Forest for determining the profile of the noninductive currents in the plasma [4]. Maintaining beam heating during the FWCD phase also provides information on the ion temperature and the poloidal fields through the charge exchange recombination and motional Stark effect diagnostics.

The FWCD system has been extended by adding two 2 MW transmitters which have a frequency range of 30–120 MHz to the 2 MW 30–60 MHz system. The experiments described have typically 2–3 MW of power coupled to the plasma, with a third of the power at 60 MHz and the remainder at 83 MHz. The antennae are three phased arrays of four current-carrying straps each, with phasing between adjacent straps of $\pi/2$. The parallel index of refraction of the coupled power is ~ 5 for both systems.

2. FAST WAVE CURRENT DRIVE IS CONSISTENT WITH THEORY

Driven currents have become larger as we have increased the fast wave power. Fast wave driven currents (not counting the bootstrap current) up to 275 kA have been generated in non-sawtoothed discharges with weak negative shear. The driven current is analyzed using a time sequence of magnetic reconstructions to determine the profiles of total current density and toroidal electric field, and the noninductive current density is found by subtracting the inductive current density from the total current density assuming neoclassical resistivity [4]. Noninductive current densities from similar discharges with co-current drive and counter-current drive are compared to eliminate the bootstrap current and neutral beam driven current, and the remainder is attributed to fast wave current drive. The profile of fast wave current so determined is shown in Fig. 1 for a discharge with 275 kA of fast wave current. Operation at 2.14 T was used to minimize absorption of waves by energetic beam ions, as discussed below. The driven current is highly localized on axis, as expected due to the strong temperature dependence of wave absorption and the higher current drive efficiency near the center, and it is in good agreement with the modeling calculations with the PICES full wave code and CURRAY ray tracing code. The peak in the driven current density is more than double the net current density in the plasma, but the driven current is partially canceled by the reverse ohmic current driven by the back-emf which appears in order to conserve flux on a resistive time scale.

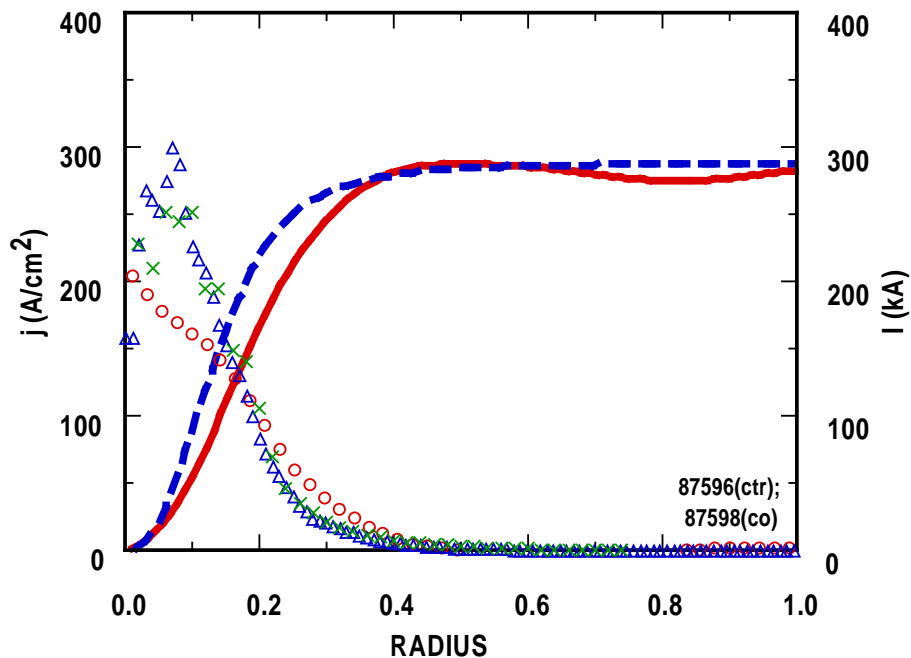


Fig. 1. The experimental profile of current density for FWCD and modeling calculations for the same case. The circles are the experimental values, the triangles are the results of a calculation using PICES, and the crosses are the results from the CURRAY code. The curves are the radial integral of experiment (solid curve) and PICES (dashed curve). The magnetic field is 2.1 T, the plasma line-averaged density is $2 \times 10^{19} \text{ m}^{-3}$, the peak electron temperature is 7 keV, and the plasma current is 1.6 MA.

In previous work [5,6] the current drive figure of merit $\eta_{fw} = n(10^{20} \text{ m}^{-3}) I(\text{MA}) R(\text{m})/P(\text{MW})$ was measured for a set of discharges with toroidal field 1 T. These are shown as the data points below 4 keV in Fig. 2. These data have been extended now to higher temperature through operation in discharges with negative central shear and VH-mode with toroidal field of 1.9 to 2.1 T and with higher fast wave power, and these data points appear in Fig. 2 above 4 keV. The higher temperature data extend the same scaling derived previously: $\eta_{fw} \propto T_e$. The data are consistent with full modeling using the CURRAY ray tracing code, which uses the measured profiles of density, temperature, and Z_{eff} to calculate the expected driven currents. The range of the CURRAY calculations is indicated by the shaded band in Fig. 2. This scaling of the figure of merit with T_e is also consistent with the simple scaling derived for ITER [7]. The calculated first pass damping for the points in Fig. 2 ranges typically from about 9% to 13%, averaging over a large number of rays representing the coupled spectrum of poloidal and toroidal wavenumbers.

Measurements made with an array of rf probes in DIII-D show that $k_t R$ is downshifted and the spectrum of the toroidal wavenumber k_t is broadened as the path length of the rays increases [8], for a broad range of conditions. However, CURRAY (and all other fast wave analysis codes) is constructed under the assumption that the

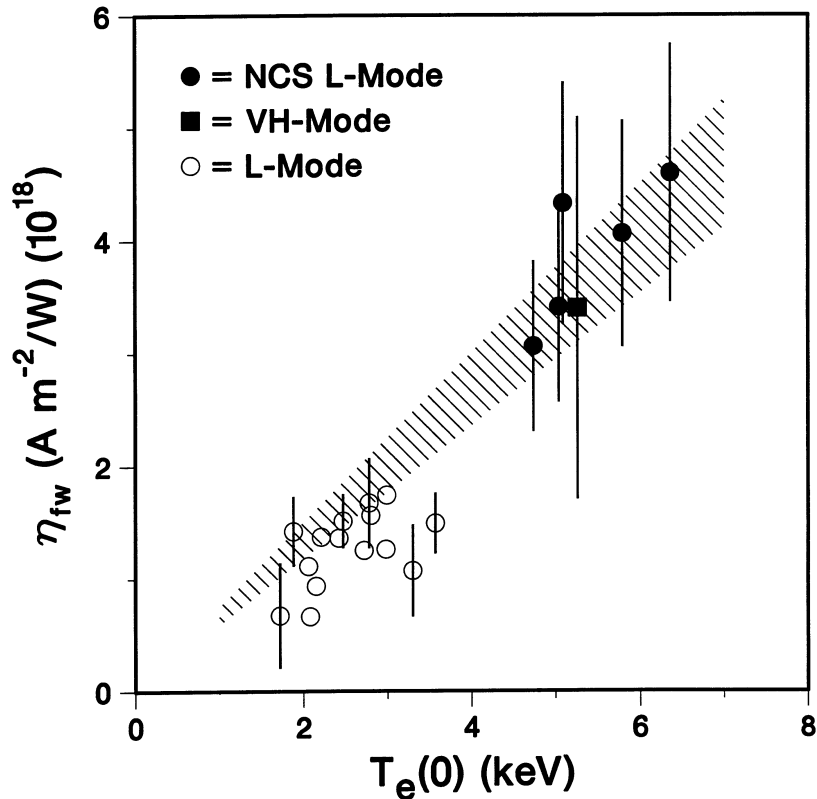


Fig. 2. The experimentally determined figure of merit η_{fw} for FWCD in DIII-D, as a function of central electron temperature. The filled circles are taken at toroidal field of $B_t = 1.9\text{--}2.1$ T in L-mode NCS or VH-mode discharges. The shaded band represents the range of modeling results using the CURRAY code on some of the discharges represented by the data points.

toroidal mode number of fast waves is conserved due to axisymmetry; i.e., $k_t R$ is constant. This makes the good agreement of η_{fw} with theory in Fig. 2 appear somewhat surprising. However, this can be resolved by consideration of the range over which n_{\parallel} changes as a ray progresses, as shown in Fig. 3(a) for a typical ray in the center of the coupled forward spectrum of n_{\parallel} , as a function of the normalized minor radius. The ray shown in Fig. 3(a) starts with n_{\parallel} of 4.8 and decays to 28% of its initial energy along the path shown. Due to the effects of the poloidal field, the n_{\parallel} gets as large as +11 and as small as -3. The wave absorption in the plasma as a function of n_{\parallel} for a large number of rays which simulate the full spectrum is plotted in Fig. 3(b). This shows that most of the power is absorbed with n_{\parallel} near 8.4, compared to an expected value of 7 from geometric upshift of the launched spectrum peaked at 5. But if the initial wave spectrum is downshifted by 25% in the ray tracing calculation, the peak in the absorption spectrum downshifts by less than 10%. This shows that the absorbed spectrum is not closely coupled to the launched spectrum due to the large variations in n_{\parallel} as the wave propagates. It also suggests that as the absorption increases at high

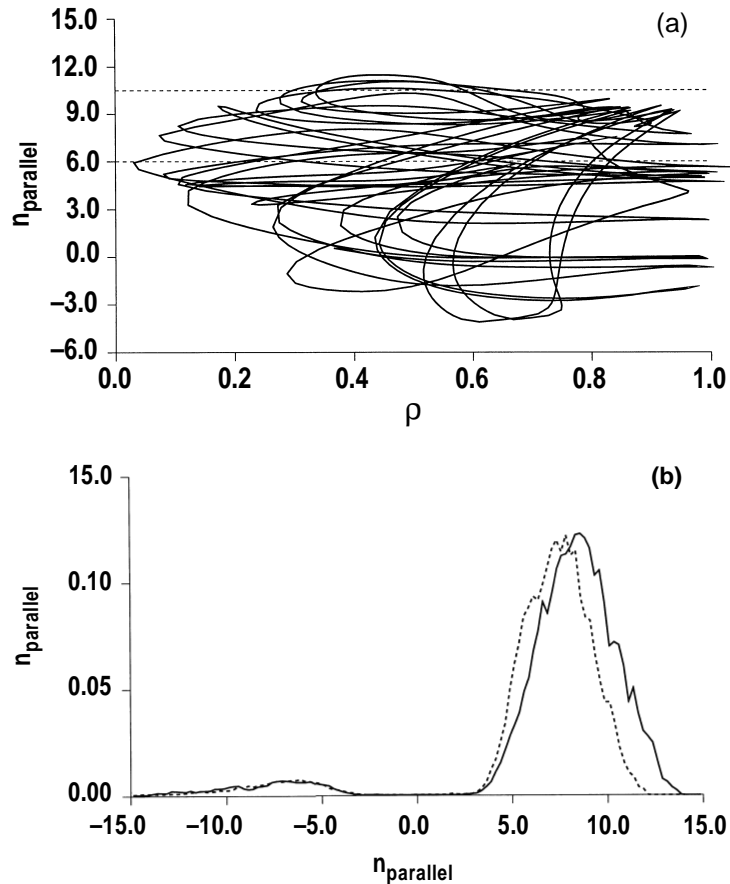


Fig. 3. (a) The parallel index of refraction as a function of normalized minor radius, as a single ray propagates on multiple passes through the plasma. The ray is launched with $n_{\parallel} = 4.8$ and frequency of 60 MHz into an L-mode plasma. (b) Power damping (arb. units) as a function of n_{\parallel} for an ensemble of 90 rays with a poloidal and toroidal spectrum corresponding to the antenna (solid line), and for a toroidal spectrum arbitrarily downshifted by 25% (dashed line). The dashed lines in Fig. 3(a) correspond to the n_{\parallel} at half the peak power damping of Fig. 3(b).

temperature and density, as for ITER, some improvement in the current drive figure of merit may be obtained by having the power absorbed at lower $n_{||}$ corresponding better to the launched spectrum.

A mechanism for loss of effective FWCD which can represent up to a third of the fast wave power is partial absorption of waves by energetic beam ions. This ion absorption has important implications for FWCD on ITER where an unthermalized population of fusion alphas is present. The evidence for beam ion absorption of the fast waves in DIII-D comes from the equilibrium reconstruction of these discharges using the EFIT code. For discharges with NBI only (no fast wave injection), the location of the magnetic axis determined in this manner is in excellent agreement with the calculated Shafranov shift using the measured thermal plasma pressure profile and the theoretical fast beam ion pressure profile. However, when 2 MW or more of FWCD is added to these NBI heated plasmas, the magnetic axis shifts outward several centimeters more than can be explained by the thermal and fast beam ion pressure profiles. In order to reconcile this discrepancy, an additional fast particle population must exist near the plasma center which can have up to 60% of the stored energy of the beam ion population. The source of this excess fast particle pressure is almost certainly energetic deuterium ions since experimentally this excess fast particle stored energy correlates with an anomalous increase in the neutron rate. A scan of the magnetic field strength from 1.6 to 2.1 T at fixed NBI power determined that the excess fast ion stored energy was largest at 1.9 T; at this field, the sixth harmonic cyclotron resonance of deuterium passes through the magnetic axis for the main FWCD frequency of 83 MHz. The excess fast ion stored energy was also found to increase as the NBI power was increased. The most plausible mechanism for this excess energetic deuterium population is high harmonic ion cyclotron absorption of the fast waves by the fast beam ions. Modeling of this process using the CQL3D Fokker-Planck code is underway. It appears that careful adjustment of the discharge parameters is necessary to avoid excessive losses to fast ions and that some loss may be unavoidable.

3. COUNTER-FWCD EXTENDS NEGATIVE CENTRAL SHEAR

FWCD has a strong heating effect in NCS discharges. Figure 4 shows data from a discharge with NCS with 3.7 MW of neutral beam heating starting at 0.35 s and 2.2 MW of coupled fast wave power with the antennas phased for counter-current drive. The electron density is low for this discharge, rising gradually from $1.0 \times 10^{19} \text{ m}^{-3}$ at the start of the fast wave pulse to 1.6 at the end, and the electron temperature rises from 3.5 keV to 6 keV. The stored energy also rises gradually, nearly doubling over the duration of the fast wave power, as shown in Fig. 4(b). The radiated power remains fixed at 1 MW throughout this period. The current driven by fast waves is 200 kA in this discharge. This is about 80% of the theoretically expected value, with the deficit presumably due to absorption of fast waves by beam ions.

The central counter-current driven by FWCD has a strong effect on the current profile in the discharge illustrated in Fig. 4. Figure 4(i) shows the central safety factor q for this discharge and for one with co-current drive. With co-FWCD, q drops to unity at 1.6 s, as verified by the start of sawtooth activity visible in the central temperature in Fig. 4(e). With counter-FWCD, the safety factor is held above unity for 0.75 s longer, until 2.35 s. No sawteeth are present until that time. Concurrently, the negative shear is strengthened by the counter-FWCD. The quantity $q(0) - q_{\min}$ is plotted in Fig. 4(h) as a measure of the magnitude of the shear reversal. The NCS configuration

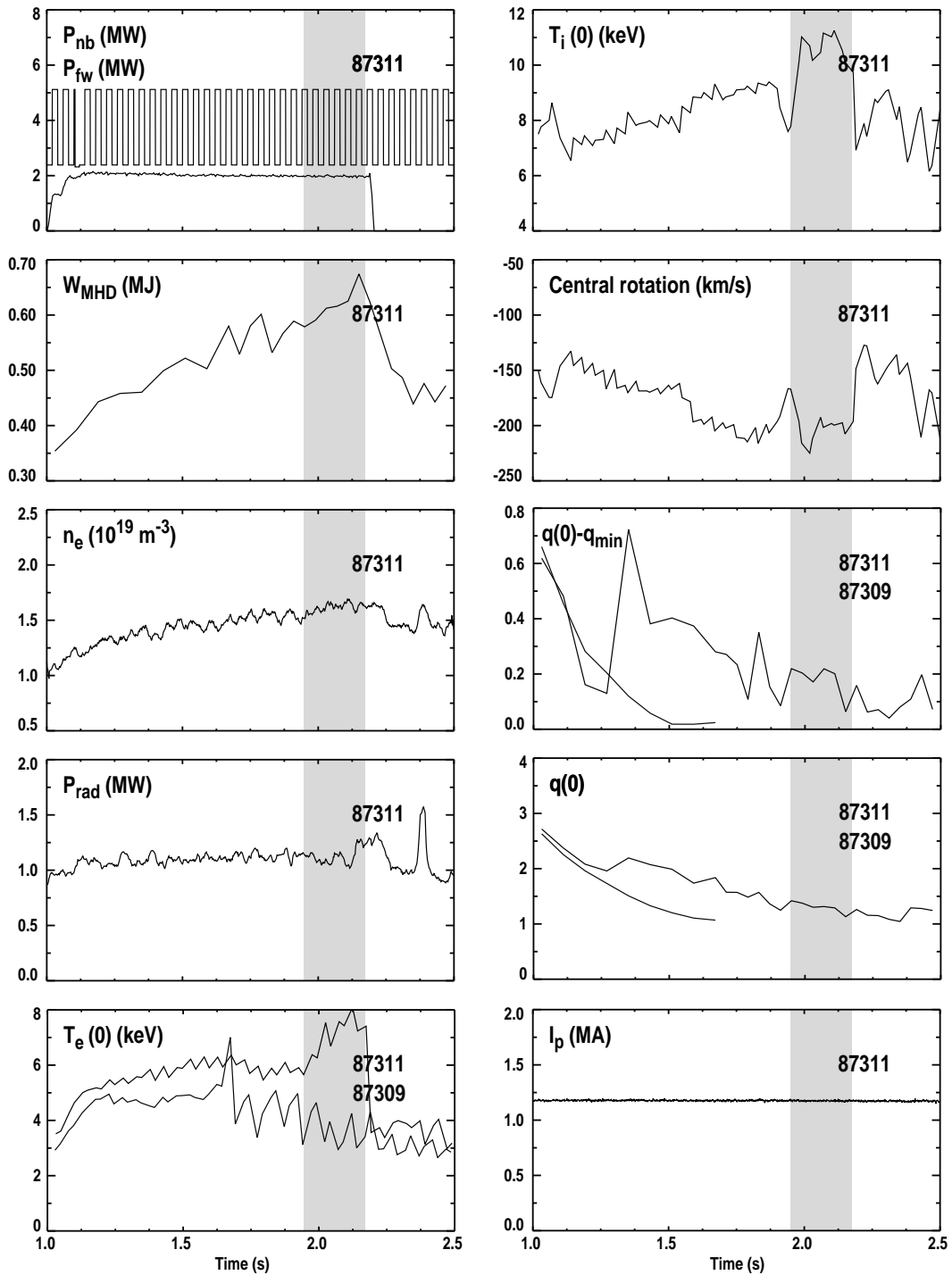


Fig. 4. Time history for a discharge with NCS and counter-FWCD. (a) neutral beam and fast wave power, (b) plasma stored energy, (c) line averaged density, (d) total radiated power, (e) peak electron temperature from ECE, (f) ion temperature from CER, (g) core rotation from CER, (h) $q(0)-q_{min}$, (i) $q(0)$, (j) plasma current. Data from a similar discharge but with co-FWCD are shown as the lower curves in (e), (h), and (i). The toroidal field is 1.9 T.

is maintained for much longer with counter-FWCD than with co-FWCD. For steady-state maintenance of the NCS configuration, it is preferable to use an off-axis co-current drive technique like electron cyclotron current drive, rather than counter-FWCD which is always central, as modeling shows that with central counter-current drive it is difficult to maintain the central safety factor above unity on a long time scale.

Some discharges show a spontaneous transition to enhanced confinement when the current profile relaxes to weak negative shear with FWCD used to provide counter-current drive and central electron heating [9]. This can be seen in the discharge of Fig. 4 at 1.95 s, nearly one second after the start of the fast wave power. At the transition, the electron temperature increases from 6 to 8 keV, the ion temperature also increases by 2 keV, and the density profile peaks slightly. The q-profile exhibits negative shear before and during the phase of enhanced performance, which ends when the minimum of q becomes unity and the sawteeth start. Transport analysis shows that the central electron thermal diffusivity decreases by a factor 2 after the transition, while ion thermal transport decreases by a factor 3 to 5. The cause of the transition is believed to be stabilization of MHD modes by the negative shear, which permits the plasma pressure and rotation to gradually build up sufficient flow shear to stabilize microturbulence [9].

4. HIGH FAST WAVE POWER WAS COUPLED TO ELMING DISCHARGES

An important requirement for a fast wave system is that power be coupled efficiently to H-mode discharges with edge localized modes (ELMs), as some of the advanced tokamak scenarios are such cases. The ELMs transiently increase the electron density at the edge which results in a significant increase in the antenna loading, which in turn causes a substantial increase in the reflection coefficient of the antennas. Were this reflected power all to return to the transmitter, the transmitter would fault.

The transmission system [10] of the FWCD system on DIII-D incorporates a decoupler [11] in conjunction with a hybrid power splitter, a combination which greatly ameliorates the effect of large reflections caused by ELMs [12]. The hybrid splitter acts to divert reflections which are uniform across the four strap antenna (as apparently are those due to ELMs) to the dummy load when the system is phased for directed current drive operation. Power is effectively coupled to the plasma between ELMs and passively diverted from being reflected to the transmitter during ELMs.

High average power can be coupled to ELMing plasmas using this system. An ELMing H-mode discharge in which 3 MW of peak fast wave power is coupled is illustrated in Fig. 5. The H-mode is triggered at 1500 ms by an elongation ramp in this high- ℓ_i experiment. Fast wave power is injected into the H-mode phase. The ELMs are indicated by the peaks in the D_α trace. The time averaged fast wave power coupled to the plasma throughout the pulse is 2.6 MW, or 85% of the peak coupled power. Figure 5(b) displays with expanded time scale the reflection coefficient at the 60 MHz generator. The coupled power from this generator remains high on average throughout significant ELM activity.

5. CONCLUSIONS

The current driven by fast waves has been extended to 275 kA in discharges with negative central shear and neutral beam heating. The current drive efficiency is consistent with theory, using a full wave code or a ray tracing code. While probe measurements show that the assumption built into the codes that the toroidal mode

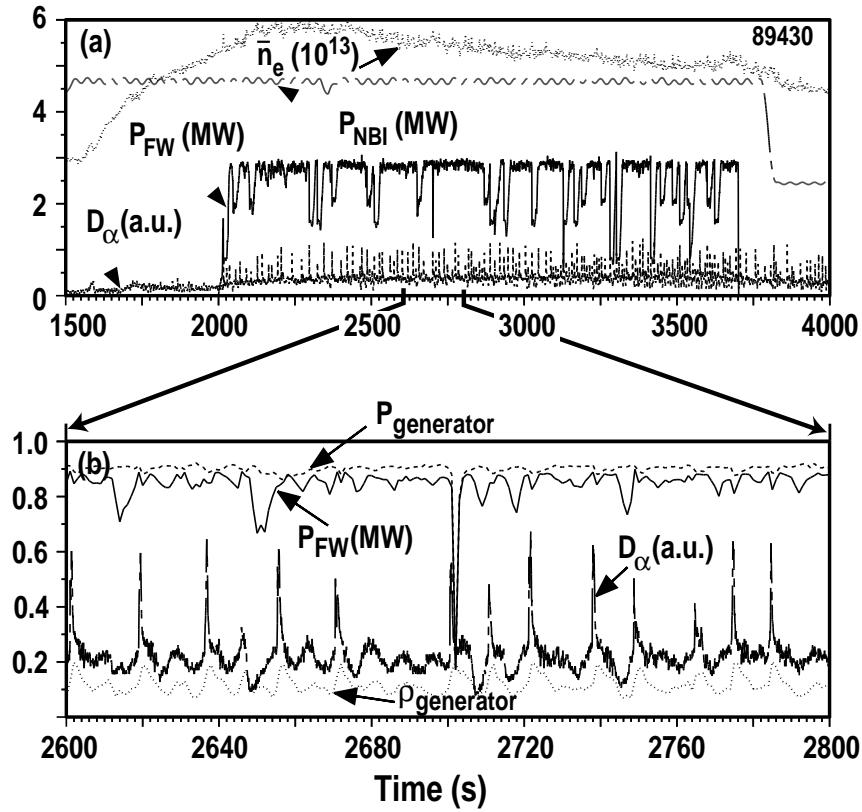


Fig. 5. 3 MW of peak fast wave power coupled to an ELMing H-mode discharge in DIII-D. (a) Injected fast wave power P_{FW} (MW), injected neutral beam power P_{NB} (MW), line averaged density \bar{n}_e (10^{19} m^{-3}), and divertor D_α light emission. (b) Expanded time trace showing coupled fast wave power from the 60 MHz generator, P_{FW} (MW), D_α , and the reflection coefficient at the generator $P_{generator}$.

number of the waves is conserved is not fully valid, the calculations show that the wave power is absorbed at the largest $n_{||}$ experienced by the wave, so the absorbed spectrum is not very sensitive to the launched spectrum. Loss of wave power to energetic beam ions has been shown to affect the current drive efficiency, and studies are underway to model this process quantitatively. When counter-FWCD was applied to discharges with negative central shear, the negative shear was strengthened and the relaxation to sawteeth which occurs when q_{min} reaches unity was delayed, showing that FWCD can help to control the current profile in advanced tokamak discharges. Under some conditions in NCS the plasma can spontaneously make a transition into a regime of improved performance, with a reduction in both the ion and the electron heat diffusivities. Recent results show that high power FWCD can be applied even in ELMing H-mode plasmas through use of a transmission system which passively directs power reflected from the antenna to a dummy load rather than the generator.

REFERENCES

- [1] LAZARUS, E.A., et al., "Higher Fusion Power Gain With Pressure Profile Control in Strongly Shaped DIII-D Tokamak Plasmas," to be published in *Phys. Rev. Lett.*
- [2] LAZARUS, E.A., et al., *Phys. Fluids* **B3** (1991) 2220.
- [3] STRAIT, E.J., et al., *Phys. Rev. Lett.* **75** (1995) 4421; LEVINTON, F.M., et al., *Phys. Rev. Lett.* **75** (1995) 4417.
- [4] FOREST, C.B., et al., *Phys. Rev. Lett.* **73** (1994) 2444.
- [5] PINSKER, R.I., et al., in *Plasma Physics and Controlled Nuclear Fusion Research 1992, Proc. 14th Int. Conf. Würzburg* (International Atomic Energy Agency, Vienna, 1993), Vol. 1, p. 109.
- [6] PETTY, C.C., et al., *Nucl. Fusion* **35** (1996) 773.
- [7] UCKAN, N.A., et al., *ITER Physics Design Guidelines: 1989* (International Atomic Energy Agency, Vienna, 1990).
- [8] IKEZI, H., et al., *Phys. Plasmas* **3** (1996) 2306.
- [9] FOREST, C.B., et al., *Phys. Rev. Lett.* **77** 3141 (1996).
- [10] deGRASSIE, J.G., et al., *Proc. 15th IEEE Symp. on Fusion Engineering, Hyannis* (Institute of Electrical and Electronics Engineers, Inc., Piscataway, 1993) 1073.
- [11] PINSKER, R.I., et al., *Proc. 15th IEEE Symp. on Fusion Engineering, Hyannis* (Institute of Electrical and Electronics Engineers, Inc., Piscataway, 1993) 1077.
- [12] GOULDING, R.H., et al., *Proc. 11th Top. Conf. on RF Power in Plasmas, Palm Springs* (American Institute of Physics, Woodbury, New York, 1995) 397.